Journal of Solid State Chemistry **144,** 416–422 (1999)
Article ID jssc.1999.8189, available online at http://www.idealibrary.com on IDEAL®

Compressibility and Vibrational Modes in Solid As_4O_6

Andrzej Grzechnik[1]

École Normale Supérieure de Lyon, 46 allée d'Italie, 69364 Lyon Cedex 07, France; and Laboratoire de Physico-Chimie des Matériaux Luminescents, Université Claude Bernard Lyon I, 43 Bd. du 11 Novembre 1918, 69622 Villeurbanne Cedex, France

Received July 27, 1998; in revised form February 1, 1999; accepted February 2, 1999

The phonon spectrum of solid As_4O_6 (arsenolite, $Fd3m$, $Z = 8$) ambient and high pressures is studied with Raman and infrared spectroscopies and analyzed in relation to the vibrational spectrum of the adamantane As_4O_6 molecule in the vapor state. The behavior of arsenolite upon compression can be interpreted as a result of an enhancement of intermolecular interactions between two equivalent As_4O_6 molecules at T_d symmetry sites of the "primitive" unit cell. The enforced interactions between the molecules through intermolecular O···O repulsions lead to a large increase of correlation field splittings of the internal vibrations due to the predominant bending and bridge stretching deformations. Eventually, at about 6 GPa they lift degeneracies of the internal modes and lower the symmetry of the crystal lattice. The observed phase transition in solid As_4O_6 is reversible without any hysteresis.

INTRODUCTION

The structure of solid As_4O_6 (arsenolite, $Fd3m$, $Z = 8$, $T_m = 547$ K) is obtained by putting the adamantane As_4O_6 molecule into the position of carbon atoms in the diamond lattice, the intermolecular O···O distance being equal to 3.022 Å (1–3). The other two polymorphs of As_2O_3 are related to As_2S_3 orpiment: As_2O_3 claudetite(I) ($P2_1/n$, $Z = 4$, $T_m = 587.5$ K) and As_2O_3 claudetite(II) ($P2_1/n$, $Z = 4$, $T_m = 583.5$ K) (3–6). Claudetite(I), claudetite(II), and orpiment have similar puckered-layered structures, in which a 6^3 net of As atoms is joined through the X(X: O, S) atoms. They differ in the arrangement of the As atoms above and below the mean plane of the X atoms. Arsenolite is obtained from a vapor phase or from solutions (1). Its formation depends on kinetic factors, since claudetite(I) is the thermodynamically stable phase at ambient pressure and room temperature. The irreversible transformation of arsenolite into claudetite(I), catalyzed by water, occurs at 453 K (1). The reversibility of the arsenolite → clauditite reaction is facilitated by shear stress (7). Further reversible (I) → (II) transition in claudetite takes place at 513 K (4).

Amorphous As_2O_3 can be prepared by either As_4O_6 vapor deposition or by cooling the As_2O_3 melt (1). Neutron diffraction (8) and infrared (9) studies of the structure of vitreous As_2O_3 disagree with each ohter. According to Clare *et al.* (8), the neutron data confirms the presence of three-membered rings of AsO_3 units similar to those in the As_4O_6 molecule, the basic building block in arsenolite. From comparison of the IR spectrum of the glassy form with those of the cubic and monoclinic polymorphs, Lezal and Konak (9) concluded that the structure of amorphous As_2O_3 is related to disordered claudetites. However, they did notice that the As_2O_3 glass recrystallizes into arsenolite. On the other hand, the Raman spectrum of vitreous As_2O_3 can be explained with a dynamical model assuming various disordered domains related to both the three-dimensional arsenolite and layered claudetite-like structures (10–15).

Adamantane-like building blocks are present in numerous inorganic solids. They can also be found in the cubic forms of antimony and bismuth trioxides, that along with arsenic and phosphorus trioxides are examples of inorganic cage structures and prototype solid state systems (3). P_4O_{6+n} molecules ($n = 0$–4) and solid ($n = 1$–4) possess the adamantane cages with additional oxygen atoms ($n = 1$–4), that are localized in peripheral positions and linked to the cages through pentavalent phosphous atoms (16–18). These terminally bound oxygens can be substituted by chalcogens (S, Se) (19) or organic azides (20). Compressibility and vibrational modes of molecular solids are of intrinsic interest because they provide a convenient way to investigate "internal" modes of the molecules embeded in a crystal matrix, along with the "external" oscillations derived from hindered translations and rotations of the molecular units. Studies within a series of related solids could provide invaluable information on the response of structures and chemical bonding to external pressure. This is especially important for the synthesis of semiconducting crystalline and amorphous materials in the mixed oxide systems based on phosphorus, arsenic, and vanadium (21, 22) utilizing high-pressure

[1]Currently at Max-Planck-Institut für Festkörperforschung, Heisenbergstrasse 1, D-70569 Stuttgart, Germany.

0022-4596/99 $30.00

techniques (23). In this study, the phonon spectrum of solid As_4O_6 at ambient and high pressures is analyzed in relation to the vibrational spectrum of the As_4O_6 molecule in the vapor state. The combined use of infrared spectroscopy in the FAR- and MID-regions (below and above about 500 cm^{-1}, respectively) and Raman spectroscopy to investigate a high-pressure behavior of a molecular solid is presented for the first time.

EXPERIMENTAL

Polycrystalline sample of arsenolite was prepared by recrystallization of the As_2O_3 starting material (1), purchased from Aldrich. Raman spectra, with spectral resolution of about 2 cm^{-1}, were collected using an XY Dilor Raman spectrometer (1800 groove/mm grattings) in backscattering geometry with CCD signal detection. Raman scattering was excited using an Ar^+ laser at a wavelength of 514.5 nm. Infrared measurements were performed on a Bruker 113v instrument. The transmittance spectra in the 200–700 cm^{-1} range were collected using a Mylar beam splitter (6 mm), Si bolometer detector, and ceramic global source. The run conditions were: 128 scans with spectral resolution 4 cm^{-1} and a spectral aperture open to 10 mm. The transmittance spectra in the 500–1700 cm^{-1} range were collected using a Ge-coated KBr beamsplitter, DTGS detector with a KBr window, and ceramic globar source. The run conditions were: 2048 scans with spectral resolution 4 cm^{-1} and a spectral aperture open to 10 mm. During all the high-pressure experiments, the sample and the pressure transmitting medium CsI, both carefully dried, were loaded into a Mao–Bell-type diamond cell with type II-a diamonds, brilliant cut with 600-mm culets, and a sample chamber diameter of 250 mm. Pressures were determined from the R_1 ruby fluorescence line (24). For both series of infrared measurements, carried out without any additional beam condensing optics, the reference spectra were collected through a gasketed diamond cell loaded only with CsI and ruby chips.

RESULTS AND DISCUSSION

The free M_4O_6 molecule (M: P, As) has T_d point group symmetry and can be pictured as four M atoms in a cage tetrahedral arrangement, interconnected by six O atoms at the vertices of an octahedron with each oxygen atom equidistant from its two M neighbors (2, 17, 25). The internal vibrations of this molecule the $\Gamma_{int} = 2A_1 + 2E + 2F_1 + 4F_2$, where the A_1 and E modes are Raman active only, while the F_2 modes are both Raman and infrared active. The rotational and translational modes are $\Gamma_{rot} = F_1$ and $\Gamma_{trans} = F_2$, respectively. The Raman and infrared frequencies of the internal modes in the As_4O_6 vapor were measured and assigned by Brumbach and Rosenblatt (26) and Konings *et al.* (25) (Table 1).

TABLE 1
Observed Vibrational Bands (cm^{-1}) in Vapor and Solid Phases of As_4O_6 at Ambient Pressure

Vapor	Solid
Internal modes	
$A_1(\nu_1)$: 555[a]	A_{1g}: 559; A_{2u}: n.a.
$A_1(\nu_2)$: 381[a]	A_{1g}: 368; A_{2u}: n.a.
$E(\nu_3)$: n.o.[a]	E_g: n.o.; E_u: n.a.
$E(\nu_4)$: 185[a]	E_g: 182; E_u: n.a.
$F_1(\nu_5)$: n.a.	F_{1g}: n.a.; F_{2u}: n.a.
$F_1(\nu_6)$: n.a.	F_{1g}: n.a.; F_{2u}: n.a.
$F_2(\nu_7)$: 833.2[b]	F_{2g}: 780; F_{1u}: 793
$F_2(\nu_{10})$: 495.6[b]	F_{2g}: 469; F_{1u}: 480
$F_2(\nu_9)$: 372.9[b]	F_{2g}: 413; F_{1u}: 340
$F_2(\nu_8)$: 255.0[b]	F_{2g}: 266; F_{1u}: 255
Rotational/librational modes	
F_1: n.a.	F_{1g}: n.a.; F_{2u}: n.a.
Translational modes	
F_2: n.o.	F_{2g}: 82; F_{2u}: acoustic

Note. n.a., not active; n.o., not observed.
[a]Ref. (26).
[b]Ref. (25).

Figure 1 shows calculated atomic displacements for the F_2 modes in the As_4O_6 "free" molecule, using a valence force field (27) comprised of the terms due to the As–O stretching, O–As–O bending, As–O–As bending, As–O/O–As–O stretching–bending interaction, As–O/As–O–As stretching–bending interaction, and O–As–O/As–O–As bending–bending interaction. The refined force terms from the starting values given for the As–O stretching (31) N/m), O–As–O bending (3.2 N/m), and As–O–As bending (2.3 N/m) by Lucovsky and Galeneer (10) are 37.97, 10.92, 7.92, 2.26, 5.04, and 0.00 N/m, respectively. The calculated wavenumbers in cm^{-1} are: 543 (A_1), 357 (A_1), 478 (E), 216 (E), 836 (F_2), 508 (F_2), 368 (F_2), and 259 (F_2). As seen from the comparison of the calculated values with the values observed by Brumbach and Rosenblatt (26) and Konings *et al.* (25) (Table 1), the agreement is reasonable, taking into account the fact that the measured wavenumbers come from two different data sets. The ν_7 (833.2 cm^{-1}), ν_{10} (495.6 cm^{-1}), ν_9 (372.9 cm^{-1}), and ν_8 (255.0 cm^{-1}) modes in the notation given by Konings *et al.* (25) can be attributed to the predominant As–O stretching vibrations, O–As–O bridge stretching, As–O–As bridge stretching, and As–O–As bending oscillations, respectively. Similar assignment of the F_2 modes was proposed earlier for P_4O_6 (17, 28).

In the primitive unit cell of solid As_4O_6 derived from the face-centered one ($Fd3m$, O_h^7, $Z = 8$) (2), the two equivalent As_4O_6 molecules occupy the T_d symmetry sites, with the intermolecular O···O distance equal to 3.022 Å. The internal modes in arsenolite are distributed as $\Gamma_{int} = 2A_{1g} + 2E_g + 2F_{1g} + 4F_{2g} + 2A_{2u} + 2E_u + 2F_{2u} + 4F_{1u}$, where the A_{1g}, E_g, and F_{2g} modes are Raman active, while the

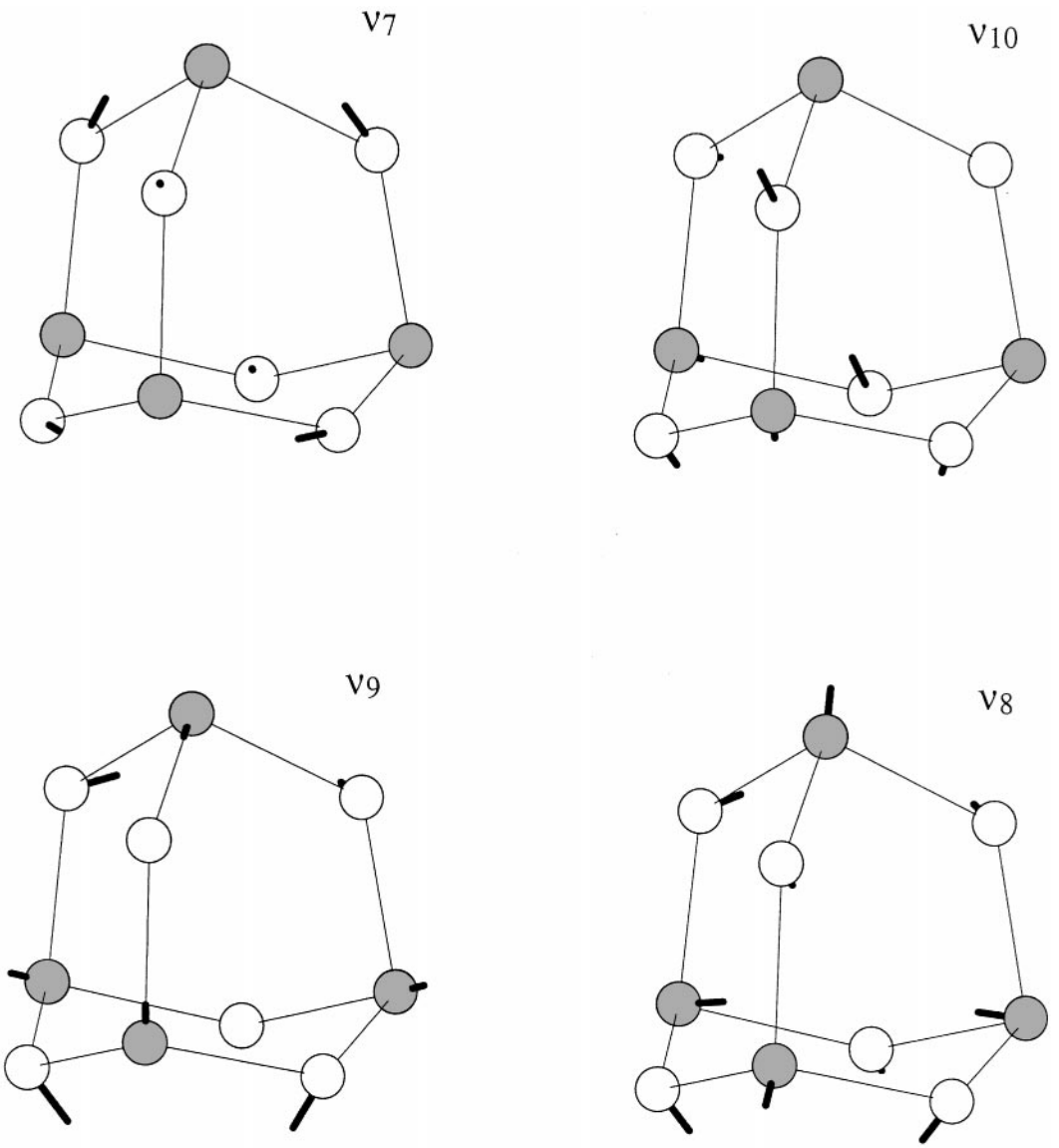

FIG. 1. Atomic displacements (ticks) for the F_2 modes in the As_4O_6 molecule. Filled symbols are the As atoms and open symbols are the O atoms. The lengths of the ticks indicate relative magnitudes of the atomic displacements from equilibrium.

F_{1u} modes are infrared active. The librational, translational, and acoustic modes are $\Gamma_{lib} = F_{1g} + F_{2u}$, $\Gamma_{trans} = F_{2g}$, and $\Gamma_{acoustic} = F_{1u}$, respectively. The correlation of the modes in As_4O_6 from a "free" molecule into a crystal demonstrates that the only optically active "external' translational mode in the solid should be observed in its Raman spectrum, while all four infrared active modes are the internal modes (Table 1). The correlation field splitting of the F_{2g} and F_{1u} vibrations in the crystal originates from a wavenumber separation of the infrared active (out-of-phase) and Raman active (in-phase) components of the same F_2 internal modes of the "free" molecule (Fig. 1).

The observed Raman spectrum in this study (Table 1, Fig. 2) is in agreement with the measurements by Beattie *et al.* (29), who used single-crystal polarization data to assign the fundamentals of the As_4O_6 crystal as F_{2g}: 268, 470, 780 cm^{-1}; E_g: 184 cm^{-1}; A_{1g}: 370, 560 cm^{-1}. The band at 82 cm^{-1} was assigned to the translational mode by Brumbach and Rosenblatt (26). The weak Raman band at 413 cm^{-1} (Table 1, Fig. 2), previously ambigously attributed to the E_g type (26, 29), is in fact the internal F_{2g} mode, based on its pressure dependence (see below). There are only four observed infrared bands in solid As_4O_6 (Table 1, Figs. 3 and 4) as predicted by factor group analysis (the shoulder features between 500 and 550 cm^{-1} are artifacts due to the very low transmission of the Mylar beam splitter at this wavenumber range). Remarkable differences, including the number of bands, were found in earlier infrared transmission

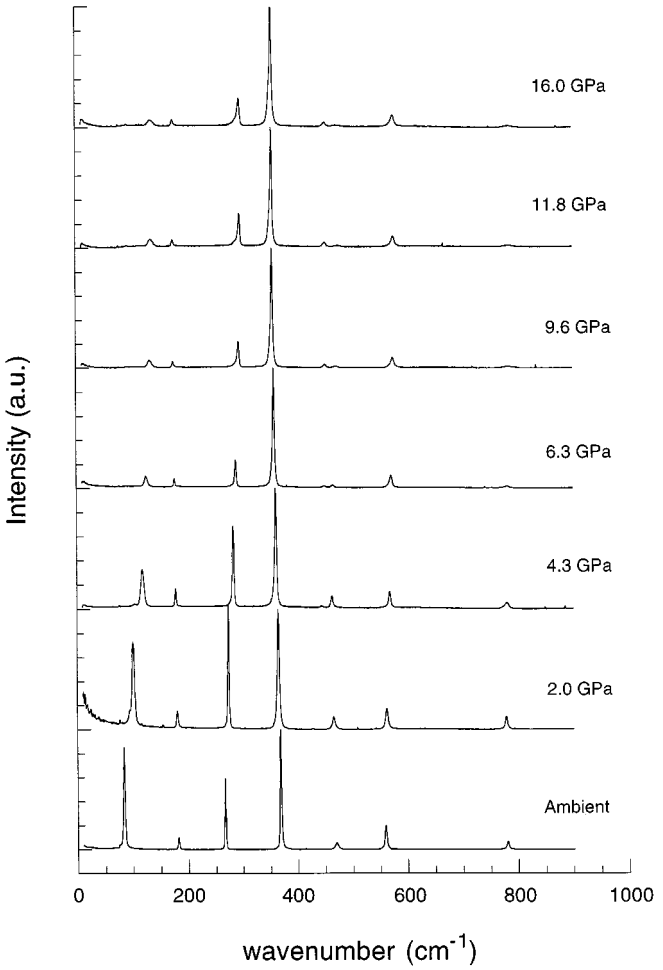

FIG. 2. Raman spectra of solid As_4O_6 as a function of pressure.

studies of arsenolite, dependent on whether nujol mull slurries or KBr pellets were used to measure the spectra (9). The infrared spectrum of solid As_4O_6 is very similar to the fundamental one of the "free" molecule (25), providing that the high purity sample and dry CsI solid solvent are used for data collection (Table 1, Figs. 3 and 4). The presence of a weak $\nu_7 + \nu_8$ combination band, visible in the infrared spectrum of the As_4O_6 vapor above 558 K (25), can be obscured in the spectra of this study due to the interference fringes from multiple reflections of the infrared light between diamond culets (Fig. 4).

Raman spectra of arsenolite were measured up to 16 GPa (Figs. 2 and 5). Upon compression, the ν_2 mode (A_{1g}) at 368 cm^{-1} and the ν_4 mode (E_g) at 182 cm^{-1} shift to lower wavenumbers. The ν_4 mode and the ν_8 mode (F_{2g}) at 266 cm^{-1} split into two components at above 6 GPa (lifting of mode degeneracy). When pressure is applied, the band at 413 cm^{-1} shifts upward in wavenumbers, while the band at 469 cm^{-1} shifts downward. These two bands are heading into a collision at about 6–8 GPa. The crossing, however, does not occur and the two bands repel each other with the lower wavenumber band gaining intensity from the higher wavenumber band. Such a behavior can be explained by the same symmetry of the two separate modes. In previous studies, the band at 413 cm^{-1} was questionably assigned to the E_g symmetry type (26, 29). However, based on its pressure dependence, it is rather of the F_{2g} type corresponding to the As–O–As stretching ν_9 oscillation. The splitting of the ν_4 and ν_8 modes, and the avoidance of crossing for the ν_9 and ν_{10} modes at about 6–8 GPa are an indication for a pressure-induced structural change in the molecular lattice of solid As_4O_6. In addition, a very weak new band is observed at about 80 cm^{-1} above approximately 12 GPa, that, along with the band at 82 cm^{-1} already observed at ambient conditions, can be assigned to the translational modes of the As_4O_6 molecule. This band is probably too weak in intensity to be observed at lower pressures, at around 6 GPa. As seen from the results of factor group analysis, there is only one external mode optically active in the cubic lattice of arsenolite.

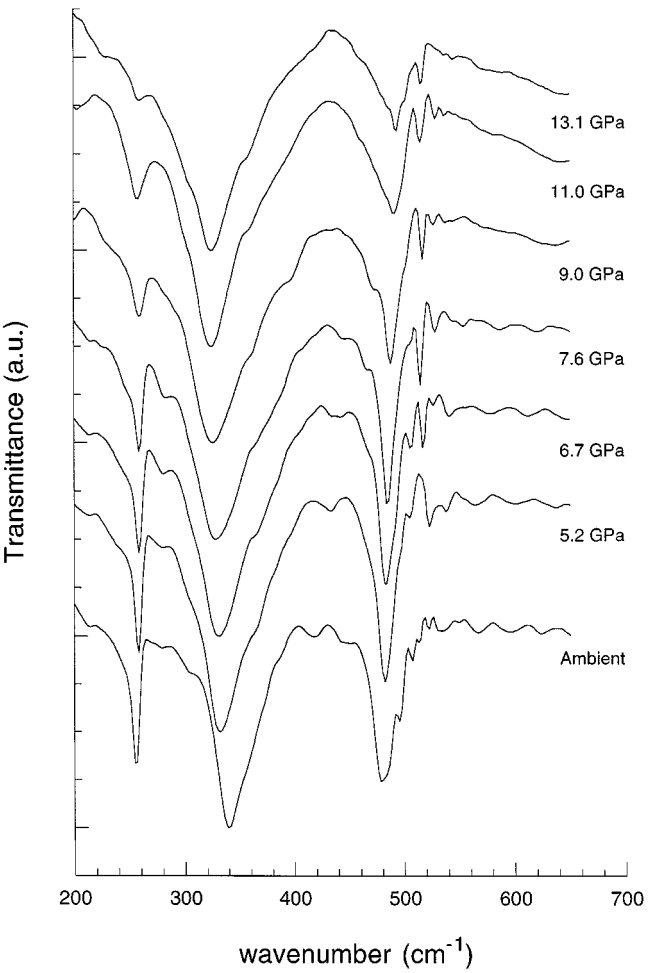

FIG. 3. Far-infrared spectra of solid As_4O_6 as a function of pressure.

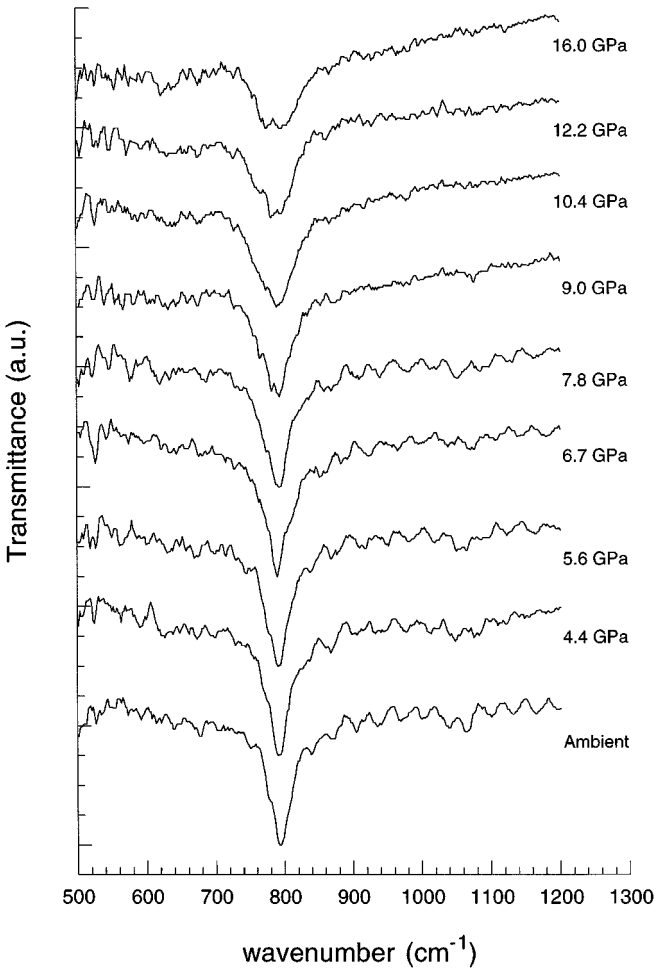

FIG. 4. Mid-infrared spectra of solid As_4O_6 as a function of pressure.

Infrared transmission spectra of solid As_4O_6 in the 500–1200 cm^{-1} and 100–700 cm^{-1} wavenumber ranges were recorded up to 13.1 and 16.0 GPa, respectively (Figs. 3, 4, and 6). At ambient and near-ambient pressures, the ν_8 band at 255 cm^{-1} resembles a reflectance feature and, unlike its Raman active counterpart, does not split into two bands upon further compression. Instead, it broadens and becomes more symmetric as a result of an increase of the mode damping. Similar behavior is observed for the ν_{10} and ν_9 bands. It is remarkable that these two bands diverge with increasing pressure and the ν_9 band due to the As–O–As stretching mode shifts to lower frequencies. At pressures up to about 7 GPa, the principal ν_7 band slightly decreases in wavenumbers and eventually splits into two components at about 8 GPa with the lower wavenumber and exhibiting a negative pressure shift. It is to be noted that all the pressure-induced changes observed both in Raman and infrared spectra are reversible with no hysteresis.

The internal modes are sensitive to changes in environment perturbations of a molecule in a crystal. Correlation field splitting (Davydov splitting) effects are due to long-range interactions with internal vibrations of equivalent molecules in the same unit cell of a crystal (30). This field leads to a wavenumber separation of the infrared and Raman active components of the same internal modes. These interactions may be largely affected by pressure, since their potential energy, dependent on whether the internal vibrations of equivalent molecules in the unit cell are in phase (Raman active modes) or out of phase (infrared active modes), could change during compression. Using Raman and infrared data on the pressure dependence of the internal modes in arsenolite with two equivalent As_4O_6 molecules in the primitive unit cell, the plot in Fig. 7 can be constructed, showing the absolute difference in wavenumbers between the infrared and Raman components of the ν_7, ν_8, ν_9 and ν_{10} internal vibrations (Fig. 1) as a function of pressure up to 6 GPa, to the onset of a pressure-induced structural transformation. It is remarkable that the Davydov splitting largely increases for the ν_8, ν_9, and ν_{10} modes assigned to the predominant As–O–As bending, As–O–As stretching, and O–As–O stretching oscillations, respectively. It is doubled on average for all these modes at 6 GPa, but it remains approximately constant for the As–O stretching ν_7 mode.

The above observations on high pressure vibrational behavior of solid As_4O_6, i.e., lifting of mode degeneracies and

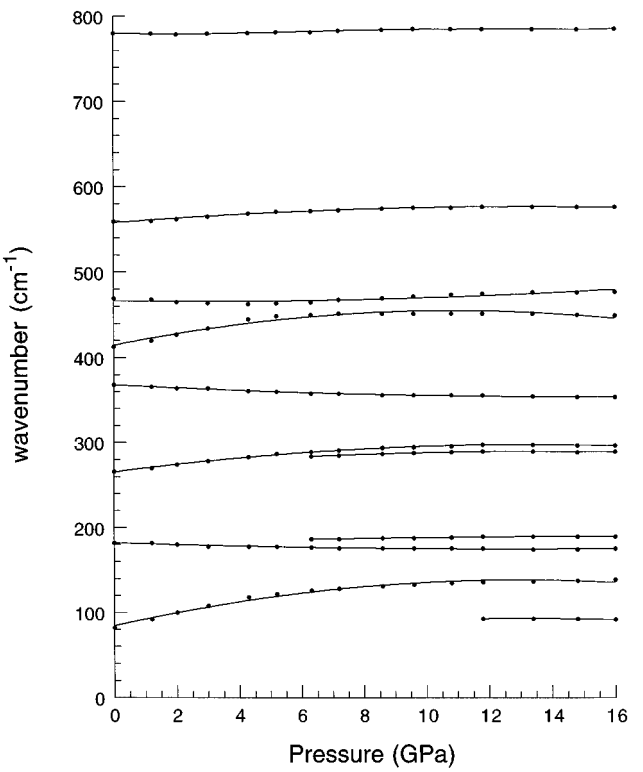

FIG. 5. Pressure dependence of Raman bands in solid As_4O_6. The error in wavenumbers is equal to the resolution for the Raman experiments, which is about 2 cm^{-1}. The lines are guides for the eyes.

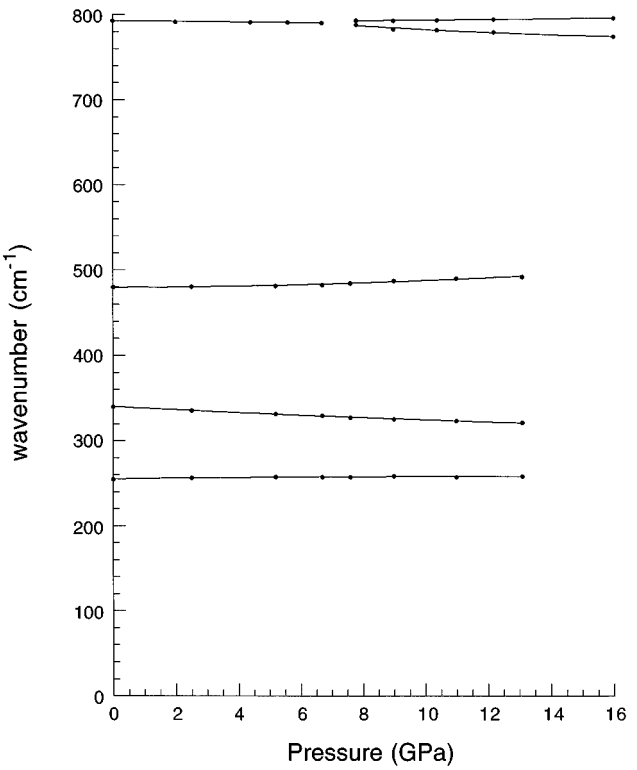

FIG. 6. Pressure dependence of infrared bands in solid As_4O_6. The error in wavenumbers is equal to the resolution for the infrared experiments, which is 4 cm^{-1}. The lines are guides for the eyes.

negative pressure shifts of some of the internal oscillations, can be interpreted as a result of an enhancement of the intermolecular interactions between the two equivalent As_4O_6 molecules at the T_d symmetry sites of the primitive unit cell ($Fd3m$, O_h^7, $Z = 8$). The largely increased Davydov splittings for the ν_8, ν_9, and ν_{10} modes are clear evidence for an internal strain of the molecules due to their bending and bridge stretching deformations under compression. The enforced interactions between the molecules through the enhanced intermolecular O···O repulsions lead to an increase of a separation between the in-phase (Raman active) and out-of-phase (infrared active) components of the internal vibrations. Eventually at about 6 GPa, they lift degeneracies of the internal modes and lower the symmetry of the crystal lattice. Such a structural change is consistent with the appearance of an additional translational oscillation of the As_4O_6 molecule. Since the distortion of the As_4O_6 crystal lattice is associated with the perturbations of the molecular environment but not with significant, if any, relative displacements of the As and/or O atoms, the observed phase transition is reversible without any hysteresis. The splitting of the internal E_g mode (ν_4) upon compression would imply the tetragonal distortion of the molecular structure, e.g., the $O_h \rightarrow D_{4h}$ point group symmetry lowering. On the other hand, lack of a drastic change in the number of the observed Raman and infrared bands would suggest that the number of molecular groups in the primitive unit cell remains constant ($Z_{\text{primitive}} = 2$), e.g., the D_{2d} symmetry site of the As_4O_6 molecules in D_{4h} point group ($T_d \rightarrow D_{2d}$).

The stability of the adamantane-like structure in solid As_4O_6 found here indicates that, unlike shear stress (7), hydrostatic (or nearly hydrostatic) compression does not facilitate the arsenolite–claudetite transformation at room temperature. This, along with the observation that crystalline and glassy As_2S_3 phases tend to increase their dimensionality under pressure (31, 32), implies that the changes in the dynamics of vitreous As_2O_3 should not be expected in the arsenolite-like disordered domains, but rather in the claudetite-like ones, in which the density fluctuates due to the conformational transitions between claudetite(I)-like and claudetite(II)-like states (14, 15). On could predict that a model assuming the presence of three-membered rings of AsO_3 units similar to those in the As_4O_6 molecule (8) would explain the structure of amorphous As_2O_3 at high pressures. This also implies that in the V_2O_5-bearing As_2O_3 amorphous systems, their semiconducting and magnetic properties

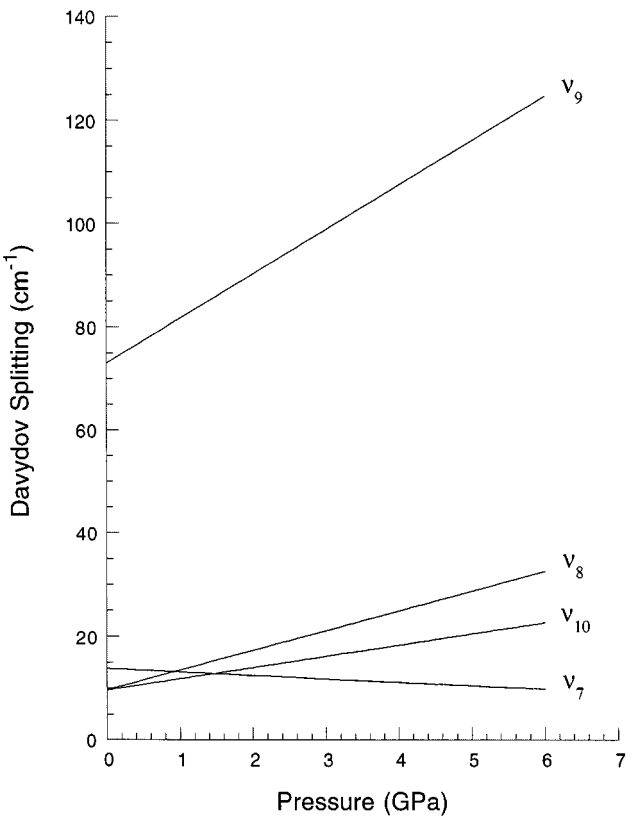

FIG. 7. Davydov splittings of the ν_7, ν_8, ν_9, and ν_{10} internal modes in solid As_4O_6 as a function of pressure. The combined error in wavenumbers is equal to the sum of the resolutions for the infrared and Raman experiments, which is about 6 cm^{-1}.

due to the presence of vanadium atoms in different valence states (21, 22) should be expected to change with increasing pressure because of local transformations in the vanadium coordination spheres (23) but not because of major changes within the As_2O_3 network. For instance, at ambient pressure the semiconducting properties arise from a hopping process of unpaired electrons between the V^{5+} and V^{4+} cations. A strong electron–phonon coupling is observed and the actual charge carriers are small polarons and their mobility depends on the thermal activation of the framework distortions and associated vibrations (33, 34). In general, the effect of high pressure on vanadium systems is an impedement of the thermally activated mobile species (23). A high-pressure study on the mixed As_2O_3–V_2O_5 systems is currently under way with a point of interest to elucidate the pressure–composition correlation of their semiconducting and magnetic properties.

ACKNOWLEDGMENTS

The sample was prepared in the Institut des Matériaux in Nantes. The infrared spectra were measured using the spectrometer at the Centre de Recherche sur les Matériaux à Haute Température in Orléans. I thank Victoria Cajipe (Nantes) and Patrick Simon (Orléans) for their hospitality and very generous help with my work.

REFERENCES

1. K. A. Becker, K. Plieth, and I. N. Stranski, *Prog. Inorg. Chem.* **4,** 1 (1962).
2. F. Pertlik, *Czech. J. Phys. B* **28,** 170 (1978).
3. A. F. Wells, "Structural Inorganic Chemistry," 5th edition. Clarendon Press, Oxford, 1984.
4. K. A. Becker, H. Karge, and I. N. Stranski, *Z. Phys. Chemie Neue Folge* **44,** (1965).
5. F. Pertlik, *Monat. Chem.* **106,** 755 (1975).
6. F. Pertlik, *Monat. Chem.* **109,** 277 (1978).
7. W. B. White, F. Dachille, and R. Roy, *Z. Kristallogr.* **125,** 450 (1967).
8. A. G. Clare, A. C. Wright, R. N. Sinclair, F. L. Galeener, and A. E. Geissberger, *J. Non-Cryst. Solids* **111,** 123 (1989).
9. D. Lezal and K. Konak, *J. Non-Cryst. Solids* **192**/**193,** 187 (1995).
10. G. Lucovsky and F. L. Galeneer, *J. Non-Cryst. Solids* **37,** 53 (1980).
11. G. N. Papatheodorou and S. A. Solin, *Phys. Rev. B* **13,** 1741 (1976).
12. G. N. Papatheodorou and S. A. Solin, *Phys. Rev. B* **13,** 1752 (1976).
13. F. L. Galeener, G. Lucovsky, and R. H. Geils, *Phys. Rev. B* **19,** 4251 (1979).
14. S. N. Yannopoulos, G. N. Papatheodorou, and G. Fytas, *Phys. Rev. E* **53,** R1328 (1996).
15. S. N. Yannopoulos, G. N. Papatheodorou, and G. Fytas, *J. Chem. Phys.* **107,** 1341 (1997).
16. M. Jansen and B. Luer, *Z. Kristallogr.* **177,** 149 (1986).
17. Z. Mielke and L. Andrews, *J. Phys. Chem.* **93,** 2971 (1989).
18. S. Strojek and M. Jansen, *Z. Naturforsch.* **52b,** 906 (1997).
19. A. R. S. Valentim, B. Engels, S. Peyerimhoff, J. Clade, and M. Jansen, *Inorg. Chem.* **36,** 2451 (1997).
20. S. Strojek and M. Jansen, *Chem. Ber.* **129,** 121 (1996).
21. E. Culea, *Phys. Status Solidi A* **126,** K159 (1991).
22. E. Culea, *J. Non-Cryst. Solids* **223,** 147 (1998).
23. A. Grzechnik, *Chem. Mater.* **10,** 2505 (1998).
24. H. K. Mao, P. M. Bell, J. W. Shaner, and D. J. Steinberg, *J. Appl. Phys.* **49,** 3276 (1978).
25. R. J. M. Konings, E. H. P. Cordfunke, and A. S. Booij, *J. Mol. Spectrosc.* **152,** 29 (1992).
26. S. B. Brumbach and G. M. Rosenblatt, *J. Chem. Phys.* **56,** 3110 (1972).
27. E. Dowty, "VIBRATZ V3.0." Shape Software, Kingsport TN.
28. R. C. Mowrey, B. A. Williams and C. H. Douglass. *J. Phys. Chem.* **101,** 5748 (1997).
29. I. R. Beattie, K. M. S. Livingston, G. A. Ozin and D. J. Reynolds, *J. Chem. Soc. A* 450 (1970).
30. P. M. A. Sherwood, "Vibrational Spectroscopy of Solids." University Press, Cambridge, 1972.
31. J. M. Besson, J. Cernogora, and R. Zallen, *Phys. Rev. B* **22,** 3866 (1980).
32. J. M. Besson, J. Cernogora, M. L. Slade, B. A. Weinstein, and R. Zallen, *Physica B* **105,** 319 (1981).
33. J. Haemers, E. Baetens, and J. Vennik, *Phys. Status Solidi* **20,** 381 (1973).
34. W. A. Harrison, "Solid State Theory." 1st ed. Dover, New York, 1980.